INSTITUTE FOR FUSION STUDIES

DOE/ET-53088-488 IFSR #488

Double Tearing Instability with Shear Flow

L. Ofman
Institute for Fusion Studies
The University of Texas at Austin
Austin, Texas 78712

March 1991

THE UNIVERSITY OF TEXAS

AUSTIN

Double Tearing Instability with Shear Flow

L. Ofman

Institute for Fusion Studies

University of Texas at Austin

Austin, Texas 78712

The linear evolution of the double tearing mode with parallel equilibrium shear flow and viscosity is investigated analytically and numerically. The dispersion relation for the growth rate of the instability with flow is derived within the framework of boundary layer theory and found to agree with numerical results in the parameter range of validity. Solutions of the incompressible time dependent linearized visco-resistive MHD equations for double tearing mode with parallel flow were found for wide relevant parameter range. Large and small rational surface separation y_s were investigated. The magnetic Reynolds number S was varied up to 10^8 and the velocity parameter V up to 0.8 of Alfven speed. The normalized wavenumber α was spanned from 0.01 (long wavelength) to 1 (short wavelength) and spatial variations of the perturbed magnetic field ψ and flow W were shown, indicating the "nonconstant-ψ" effects for small rational surface separation y_s. Centrally peaked shear flow was found to have a stabilizing effect on the double tearing mode, suppressing the growth rate linearly with V for small y_s and quadratically for large y_s. Large flow decouples the rational surfaces, reduces the growth rate, and transforms the instability to the standard tearing mode. Overstable modes were found from the solutions of the dispersion relation and in the numerical computations, their frequencies are not affected by the value of viscosity. The temporal oscillations of the solutions increase with V. For viscosity comparable or larger then resistivity a stabilizing effect was found, and in the presence of large flow the growth rate scaling approaches the standard tearing mode scaling with viscosity $\gamma_R \sim S_v^{1/6}$.

1. Introduction

The resistive tearing instability is an important phenomena in laboratory and space plasma and was first studied by Furth et. al.[1] The instability grows in a narrow layer of the plasma, where the resistivity term is dominant over the local magnetic field term in Ohm's law, allowing the field lines to break and reconnect, thus forming magnetic islands. The growth rate of the single tearing mode scales as $S^{-3/5}$ where S is the magnetic Reynolds number. The double tearing mode onsets when two such layers form close together to allow the "nonconstant-ψ" effects to enhance the growth rate γ of the instability. The analytical linear theory of tearing mode in slab geometry with equilibrium shear flow and viscosity has been considered by several authors.[2-6] They conclude that flows, which approach the Alfven velocity can greatly modify the stability criteria of single tearing instability. This was shown to hold numerically in the linear regime.[7-10]

Double tearing instability was observed in fusion devices with non monotonic current profiles in the plasma column,[11] and it is also believed to be important in solar flares.[12-13] The instability without equilibrium flow was studied by relatively few authors[14-23] and was subject to few experiments.

The effect of equilibrium flow on the double tearing mode was not considered previously, despite the fact that it can occur in fusion devices and space plasmas, and alter the behavior of the instability considerably. For instance it can partly stabilize the mode, modify the growth rate dispersion relation, and excite temporal oscillations of the perturbed quantities for relatively small shear flow (see, Secs. III-IV).

Here, the double tearing mode with equilibrium flow parallel to the magnetic field is investigated analytically and numerically. The paper is organized as follows. In Sec. II the linearized incompressible visco-resistive magnetohydrodynamic equations in slab geometry are presented, together with the initial magnetic field, flow profiles and boundary conditions that excite the double tearing mode. In Sec. III the linear growth rate dispersion relation is obtained and in Sec. IV the numerical methods and results are presented. Section V is devoted to summary of the results and discussion.

II. Model Equations

We assume that magnetohydrodynamic (MHD) theory [24] is applicable, that the plasma is incompressible with constant isotropic resistivity and constant perpendicular viscosity [25], and that gravitational effects are negligible. The basic equations in cgs units are:

$$\rho\cdot\left[\frac{\partial \mathbf{v}}{\partial t} + (\mathbf{v}\cdot\nabla)\mathbf{v}\right] = -\nabla p + \frac{1}{4\pi}(\nabla\times\mathbf{B})\times\mathbf{B} + \nu\nabla_{\perp}^{2}\mathbf{v} \tag{1}$$

$$\frac{\partial \mathbf{B}}{\partial t} = \nabla\times(\mathbf{v}\times\mathbf{B}) - \frac{c^2\eta}{4\pi}\nabla\times(\nabla\times\mathbf{B}) \tag{2}$$

$$\nabla\cdot\mathbf{v}=0, \nabla\cdot\mathbf{B}=0 \tag{3}$$

where c is the speed of light, ρ is the plasma density, $\mathbf{B}$ is the magnetic field and $\mathbf{v}$ is the velocity of the plasma. The pressure p is eliminated from the calculations by taking a curl of Eq. (1).

We use slab geometry and choose an equilibrium magnetic field of the form

$$\mathbf{B}_0(y) = \mathbf{B}_{x0}(y)\mathbf{e}_x + \mathbf{B}_{z0}(y)\mathbf{e}_z.$$

Similarly, the equilibrium plasma flow is assumed to be in the (x,z) plane aligned with the magnetic field, with the form

$$\mathbf{v}_0(y) = \mathbf{v}_{x0}(y)\mathbf{e}_x + \mathbf{v}_{z0}(y)\mathbf{e}_z.$$

Equations (1)-(3) are linearized around the magnetic field and flow velocity equilibrium solutions assuming perturbations of the form $f_1(y,t)\exp(ik_x x+ik_z z)$.

The normalized linearized time-dependent y-components of the MHD equations can be written as

$$\left(\frac{\partial}{\partial t} + i\alpha G\right)\left(W'' - \alpha^2 W\right) - i\,\alpha R^2 G'' W = i\alpha F(\psi'' - \alpha^2\psi) - i\alpha F''\psi + \frac{1}{S_v}\frac{\partial^4 W}{\partial y^4} \tag{4}$$

$$\left(\frac{\partial}{\partial t} + i\alpha G\right)\psi - i\alpha F W = S^{-1}\left(\psi'' - \alpha^2\psi\right) \tag{5}$$

where the time t is in units of Alfven time and y is in units of a_b the magnetic length scale, the primes denote derivatives with respect to y, and the perturbed physical quantities are the magnetic field $\psi = B_{y1}/B$, and flow $W = V_{y1}/V_a$ where B is a measure of the magnetic field in the plasma and V_a is the Alfven velocity. The dimensionless parameters are the magnetic Reynolds number $S = \tau_r/\tau_h$, a measure of viscosity $S_v = \tau_v/\tau_h$, the shear parameter $R = a_b/a_v$ where a_v is the shear flow length scale, and the normalized wave number $\alpha = ka_b$.

The relevant time scales in these definitions are the resistive time τ_r, the Alfven time τ_h and the viscous time τ_v given by

$$\tau_r = 4\pi a_b^2/c^2\eta \qquad \tau_h = a_b(4\pi\rho)^{1/2}/B, \quad \tau_v = \rho a_b^2/\nu .$$

The normalized equilibrium magnetic field and flow velocity components in the direction of the spatial perturbation vector **k** are given by

$$F = (k_x B_{x0} + k_z B_{z0})/kB , \qquad G = (k_x V_{x0} + k_z V_{z0})/kV_a.$$

Specifically we choose $k_z=0$, $k=k_x=\alpha/a_b$, and the following forms of F and G for the double tearing mode:

$$F(y)=1-(1+F_c)\mathrm{sech}(y), \tag{6}$$

$$G(y)=V[1-\mathrm{sech}(Ry)] ,$$

where $F_c=\cosh(y_s)-1$ is determined by the locations $\pm y_s$ where F(y) vanishes. The velocity parameter V is given in units of V_a and R is the shear parameter. The spatial dependence of F and G for V=-0.5, y_s=0.75, and R=0.5 are shown in Fig. 1. Equations (4) and (5) are solved numerically without any further approximations, subject to zero boundary conditions which are equivalent to conducting walls placed at $\pm|y_{max}|$:

$$W(-|y_{max}|)=W(|y_{max}|)=0$$

$$\psi(-|y_{max}|)=\psi(|y_{max}|)=0$$

The value of y_{max} is chosen such as to satisfy the condition $|y_{max}| \gg y_s$. When this is satisfied the results of the computations do not depend significantly on the size of the system.

III. Dispersion Relation

The growth rate of the instability is found from the time-Fourier-transformed Eqs. (4)-(5), using the boundary layer approach.[19] Upon assuming perturbations of the form $f_1(y)\exp(i\omega t+ik_x x)$ and neglecting the viscous term, these equations become

$$(\gamma + i\alpha G)\left(W''- \alpha^2 W\right) - i\,\alpha R^2 G''W = i\alpha F(\psi''- \alpha^2\psi) - i\alpha F''\psi \qquad (7)$$

$$(\gamma + i\alpha G)\,\psi - i\alpha FW = S^{-1}\left(\psi'' - \alpha^2\psi\right) \qquad (8)$$

where $\gamma=\gamma_R+i\gamma_I=i\omega\tau_h$ is the complex normalized growth rate and the subscripts R and I denote the real and imaginary parts, respectively.

The physical domain is divided in two types of regions, namely, an inner resistive region near $\pm y_s$ in which $|F|<<1$ and resistivity cannot be neglected in Ohm's law, and an ideal outer region in which the resistive term is neglected and ideal MHD equations are used ($|y|>y_s$, $|y|<y_s$).

Assuming that near the rational surfaces $\alpha^2<<d^2/dy^2$, expanding F(y) around y_s, and that the flow profile G(y) does not vary considerably near $\pm y_s$ (thus, substituting G_s=G(y)=const , G'(y)=G''(y)=0.), the inner resistive equations become

$$(\gamma + i\alpha G_s)\,\psi = (\gamma + i\alpha G_s)F'(y_s)(y-y_s)w+S^{-1}\,\psi'' \qquad (9)$$

$$(\gamma + i\alpha G_s)^2\, w'' = -\alpha^2 F'(y_s)(y-y_s)\psi'' \qquad (10)$$

where

$$w=\frac{i\alpha W}{\gamma+i\alpha G_s}.$$

In the ideal regions, the resistive term is neglected in Eq. (8), and it simplifies to $\psi=Fw$ which is then substituted into Eq. (7) to obtain

$$\frac{d}{dy}\left\{\left[(\gamma+i\alpha G)^2+F^2\right]\frac{dw}{dy}\right\}=\alpha^2\left[(\gamma+i\alpha G)^2+F^2\right]w \quad (11)$$

The above non-resistive equations describes the double kink mode with flow in slab geometry. It is solved asymptotically in terms of a power series expansion under the boundary conditions

$w(y)=w_0=\text{const}, \quad |y|<y_s,$

$w(y)=0, \quad |y|>>y_s.$

The form of Eqs. (9)-(11) is similar to those obtained in Ref. 19 for the double tearing mode without flow, therefore we generalize their solution to accommodate flow, obtaining the growth rate γ_h of the double kink mode with flow

$$\gamma_h=-\frac{\pi\alpha^3}{F'(y_s)}\int_0^{y_s} F(y')^2 dy' - i\alpha G_s \quad , \quad (12)$$

noting that the flow produces a Doppler shift in the G=0 double kink mode growth rate. Finally, we modify the dispersion relation of Ref. 19, which was derived in detail in Ref. 25, to include shear flow

$$\gamma_h=8b^{-2/3}\frac{\Gamma\left[\frac{b\cdot(\gamma+i\alpha G_s)^{3/2}+5}{4}\right]}{\Gamma\left[\frac{b\cdot(\gamma+i\alpha G_s)^{3/2}-1}{4}\right]} \quad (13)$$

where

$$b=\frac{S^{1/2}}{\alpha F'(y_s)}$$

and Γ is the complex gamma function. In the limit $G \to 0$, the results of the double tearing mode without flow are recovered in agreement with Ref. 19. When $G(y)\neq 0$ expression (13) expands to the complex plane and exhibits much more complicated behavior than the one for $G(y)=0$. The solution can have more then one branch for a given parameter set. Therefore, one needs to place additional constrains on the solutions of Eq. (13) for the growth rate. Reasonable requirements are $\gamma_R>0$, $\gamma_I\geq 0$ for growing overstable modes. Finally, the condition for small separation of singular surfaces that was used to select y_s in the numerical calculations

$$y_s<\alpha^{-7/9}S^{-1/9} \tag{14}$$

holds for the case with flow.

In the following section the results of the analytical theory were compared to the numerical calculations and were used as a guide for further investigations in the parameter space of the double tearing mode.

IV. Numerical Results

Since the method of solution is described in detail in Ref. 10, in this paper only a brief summary is presented. Equations (4) and (5) are solved numerically in the complex plane using an implicit finite difference scheme with a variable or fixed spatial grid. The variable grid spacing expands from a minimum of $\Delta y_{min}=10^{-3}$ near the singular surfaces to $\Delta y_{min}=0.5$ near the computational boundaries. When the computation domain is small ($|y_{max}|\leq 2$) a fixed grid with up to 500 grid points is used. The time step Δt is selected so that $\Delta t \leq \min\left(\gamma_R^{-1}, 0.2\gamma_I^{-1}\right)$, and the simulation is evolved for N time steps until only the fastest growing modes present in the solutions. Usually the number of time steps required is 100<N<500.

From the complex solutions $W(t, y)$ or $\psi(t, y)$, the growth rates are obtained in two steps. First, the real part of the growth rate γ_R is found by fitting a straight line to the logarithm of $W(t, y_0)$ (where y_0 is an arbitrary point in the domain). Next, the exponential trend is removed from the solutions and a Fast Fourier Transform (FFT) is performed on the remaining oscillatory part of $W(t, y_0)$, which thereby determines the imaginary part of the growth rate γ_I. If the modes are purely growing (no time-dependent oscillations are present), then only the first step in the above method is performed.

The results of the numerical computations are presented in Figs. 2-6. The spatial variations of the perturbed magnetic field ψ and perturbed flow W are shown in Fig. 2. In

Fig. 2a the parameters are $S=10^6$, $\alpha=0.5$, $V=-0.1$, $R=0.5$ (the value of R is not changed in Figs. 2-6), and the separation $y_s=0.75$ is large. Note the rapid variation of W across the two tearing layers and the location of the sharp peaks that indicate the width of the resistive regions. It has been found that large viscosity reduces the sharpness of the peaks and widens the effective resistive region widths ε, which is compatible with the single tearing mode scaling of the tearing layer width with viscous parameter as $\varepsilon \sim S_v^{-1/3}$. In Fig. 2b the separation $y_s=0.15$ is small according to condition (14) resulting in a "nonconstant-ψ" tearing mode that scales as $\gamma_R \sim S^{-1/3}$. For large flow $V=-0.5$ in Fig. 2c the double tearing mode is significantly different from the previous case: the effect of flow is evident at the external regions adjacent to the tearing layers where partial decoupling of the "nonconstant-ψ" tearing occur resulting in lower growth rate.

Analytical and numerical growth rates and their dependence on resistivity and wavenumber are presented in Fig. 3. For large flow, $V=-0.5$, small wavenumber $\alpha=0.05$ and small resistivity the computed growth rate agrees with the one obtained from Eq. (13). When $S=10^6$, $y_s=0.15$, $V=-0.5$ and the wavenumber is varied in the range $0.05 \leq \alpha \leq 1$ a very good agreement of the analytical and numerical growth rates is found.

In Fig. 4 the dependence of the growth rate γ_R on the resistivity and other parameters is shown. The solid circles correspond to computations with $\alpha=0.5$, $y_s=0.15$, the empty circles for $\alpha=0.5$, $y_s=0.75$, the solid lines for $V=-0.5$, the dashed lines for $V=-0.1$, and the triangles for $\alpha=0.05$, $y_s=0.15$. When the separation is large, $y_s=0.75$, the growth rate decreases with increasing S. Larger flow, $V=-0.5$, suppresses the growth rate further and its dependence on S approaches the standard tearing mode scaling $\gamma_R \sim S^{-3/5}$. For small separation, $y_s=0.15$, the growth rate peaks near $S=10^4$ and the stabilizing effect of large flow is more evident for $S \leq 10^4$. When the rational surface separation is of the order of the resistive layer width the growth of the double tearing mode is suppressed, while for small resistivity it scales as $\gamma_R \sim S^{-1/3}$, thus leading to the peaked behavior in Fig. 4. For $\alpha=0.05$, $y_s=0.15$, and $V=-0.5$, the values of the growth rate are an order of magnitude smaller then the for α=0.5. The main result in Fig. 4 is that the flow has a stabilizing effect on the growth rate for all calculated values of S, y_s, and α, while small y_s leads to larger growth rate due to "nonconstant-ψ" effects.

In Fig. 5 we examine the dependence of the complex growth rate on the shear flow with S=10^4 and α=0.5. When y_s=0.15 the real part of the growth rate decays almost linearly with flow while the imaginary part increases at comparable rate. When the separation is large, y_s=0.75, the effect of flow is stronger and the real part of the growth rate decays quadratically with V, while the imaginary part grows parabolically. For V=0.8 the growth rate is an order of magnitude smaller then for V=0 and the temporal oscillations dominate the behavior of the instability, in contrast to the single tearing mode with flow, Ref. 10, where the imaginary part of the growth rate was always found to be considerably smaller than the real part.

The effect of viscosity on double tearing mode with y_s=0.75, S=10^4, and α=0.5 is examined in Fig. 6. Small viscosity does not significantly affect the growth rate. When the viscosity is comparable to or larger then the resistivity a simple scaling law behavior emerges. For V=0 and V=-0.1 the scaling is $\gamma_R \sim S_v^{\,0.22}$, when V=-0.5 the double tearing mode approaches the standard tearing mode growth rate scaling with viscosity $\gamma_R \sim S_v^{\,1/6}$. This further indicates that large flow reduces the "nonconstant-ψ" effects and has a stabilizing effect. The imaginary part of the growth rate was found to be independent of viscosity, and it increases with V (see, Fig. 5).

V. Summary and Discussion

We have investigated the double tearing mode instability with shear flow, both analytically and numerically by solving the resistive MHD equations with initial equilibrium magnetic field and flow. The enhancement of the growth rate due to "nonconstant-ψ" effects in the double tearing mode was reduced by the presence of flow. For large surface separation the flow has a greater stabilizing effect then for small surface separation. Shear flow was found to induce temporal oscillations of the perturbed quantities, and the frequency of the oscillations increases with V. The overstable modes were found from the analytical dispersion relation and their values are in good agreement with the numerically obtained solutions of Eqs. (4)-(5).

The effect of viscosity in the double tearing was investigated numerically. When the viscosity is small compared to resistivity it has no significant affect on the growth rate. When viscosity is comparable or larger then resistivity, it has a stabilizing affect, and the growth rate exhibits a power law dependence on S_V. In the presence of large flow the growth rate scaling is close to the standard tearing mode scaling, namely, $\gamma_R \sim S_V^{1/6}$, and γ_I is independent of viscosity.

Double tearing instability with flow exhibits a complicated behavior in the physical and parameter space and is significantly modified by the presence of shear flow. The main result of the present work is that flow has a stabilizing effect on the double tearing instability, and thus its inclusion in fusion devices with non-monotonic current profiles can improve stability of the plasma. The invocation of the double tearing mode in explaining the much faster evolution times of the solar flares must be reviewed when shear flow is present due to its stabilizing effect.

Acknowledgments

The author would like to thank R.S. Steinolfson, P.J. Morrison and X.L. Chen for useful discussions. This work was supported by the U.S.. Department of Energy Contract No. DE-FG05-80ET-53088 and National Science Foundation Contract Nos. ATM-89-96317 and ATM-90-15705.

REFERENCES

[1]H. P. Furth, J. Killeen, and M. N. Rosenbluth, Phys. Fluids **6**, 459 (1963).

[2]X. L.Chen, and P. J. Morrison, Phys. Fluids B **2**, 495 (1990).

[3]X. L.Chen, and P. J. Morrison, Phys. Fluids B **2**, 2575 (1990).

[4]F. Porcelli, Phys. Fluids 30, 1734 (1987).

[5]R. B. Paris and W. N.-C. Sy, Phys. Fluids **26**, 2966 (1983).

[6]M. Dobrowolny, P. Veltri, and A. Mangeney, J. Plasma Phys. **29**, 303 (1983).

[7]G. Einaudi, and F. Rubini, Phys. Fluids **29**, 2563 (1986).

[8]G. Einaudi, and F. Rubini, Phys. Fluids B **1**, 2224 (1989).

[9]S. Wang, L. C. Lee, and C. Q. Wei, Phys. Fluids **31**, 1544 (1988).

[10]L. Ofman, X.L. Chen, P.J. Morrison, and R.S. Steinolfson, to appear in Phys. Fluids (1991).

[11]T.H. Stix, Phys. Rev. Letters **36**, 521 (1976).

[12]D.S. Spicer, Solar Physics **53**, 305 (1977).

[13]E. R. Priest, *Solar Magnetohydrodynamics* (Reidel, Dordrecht, The Netherlands,1985).

[14]H.P. Furth, P.H. Rutherford, and H. Selberg, Phys. Fluids **16**, 1054 (1973).

[15]D. Schnack and J. Killeen, in *Theoretical and Computational Plasma Physics,* (International Atomic Energy Agency, Viena, 1978), p. 337.

[16]Y.C. Lee, J.W. Van Dam, J.F. Drake, A.T. Lin, P.L. Pritchett, D.D'Ippolito, P.C. Liewer, and C.S. Liu, in Plasma Physics and Controlled Nuclear Fusion Research (International Atomic Energy Agency, Viena, 1979), Vol. I, p. 799.

[17]B. Carreras, H.R. Hicks, and B.V. Waddell, Nucl. Fusion **19**, 583 (1979).

[18]Yu. N. Dnestrovskii, D.P. Kostomorov, and A.M. Popov, Sov. J. Plasma Phys, 5, 289 (1979).

[19]P.L. Pritchett, Y.C. Lee, J.F. Drake, Phys. Fluids **23**, 1368 (1980).

[20]W. Kerner and H. Tasso, Plasma Phys. **24**, 97 (1982).

[21]S.M. Mahajan and R.D. Hazeltine, Nucl. Fusion **22**, 1191 (1982).

[22]V.V Gatilov, A.M. Sagalakov, and V.F. Ul'chenko, Sov. J. Plasma Phys. **15**, 31, (1989).

[23]J.F Drake and Y. C. Lee, Phys. Fluids **20**, 134 (1977).

[24]S. I. Braginskii, Rev. Plasma Phys. **1**, 205 (1965).

[25]B. Coppi, R. Galvao, R. Pellat, M.N. Rosenbluth, and P.H. Rutherford, Sov. J. Plasma Phys. **2**, 533, (1976).

Captions to Figures

Fig. 1 The initial equilibrium normalized magnetic field F(y) and shear flow G(y) for the double tearing mode with flow. The parameters are V=-0.5, y_s=0.75, R=0.5

Fig. 2 (a) The spatial dependence of the complex perturbed magnetic field ψ and flow W with V=-0.1, S=10^6, α=0.5, y_s=0.75, and S_v=10^9.

(b) Same as Fig. 2a with y_s=0.15.

(c) Same as Fig. 2a with V=-0.5, S=10^4, α=0.5.

Fig. 3 (a) Comparison of the analytical growth rate scaling vs. S obtained from Eq. (14) with the values obtained from the numerical solutions of Eqs. (4)-(5).

(b) Same as Fig. 3a for growth rate scaling vs. α.

Fig. 4 Growth rate dependence on S for several parameter values obtained from the numerical solutions of Eqs. (4)-(5).

Fig. 5 The dependence of the complex growth rate γ on the flow parameter V, and the singular surface separation y_s. The other parameters are: S=10^4, α=0.5.

Fig. 6 Growth rate scaling with viscosity parameter S_v for y_s=0.75, V=0 (dotted curve), V=-0.1 (solid curve), and V=-0.5 (dashed curve).

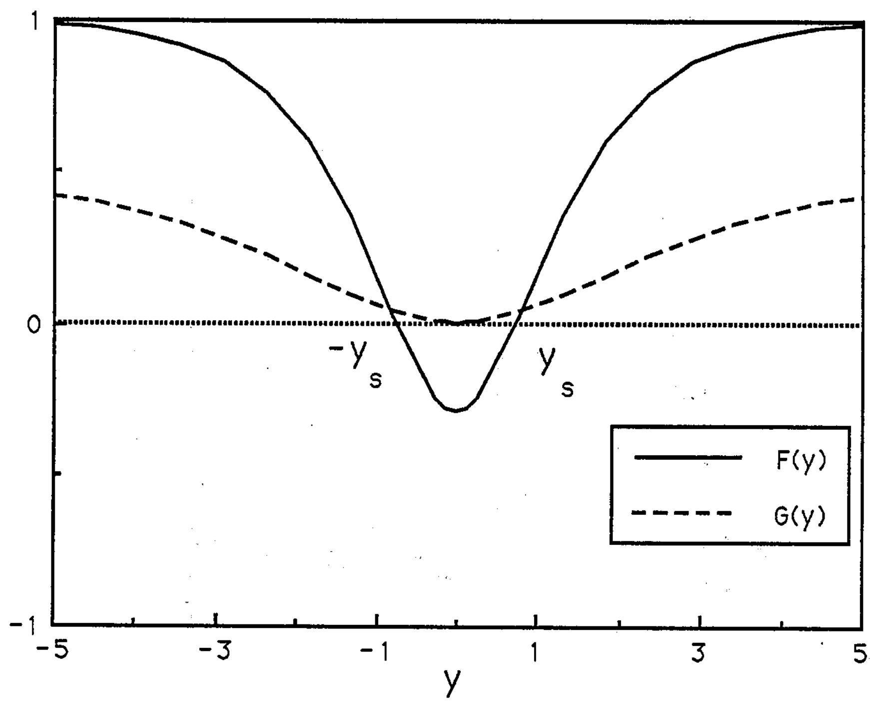

Fig. 1

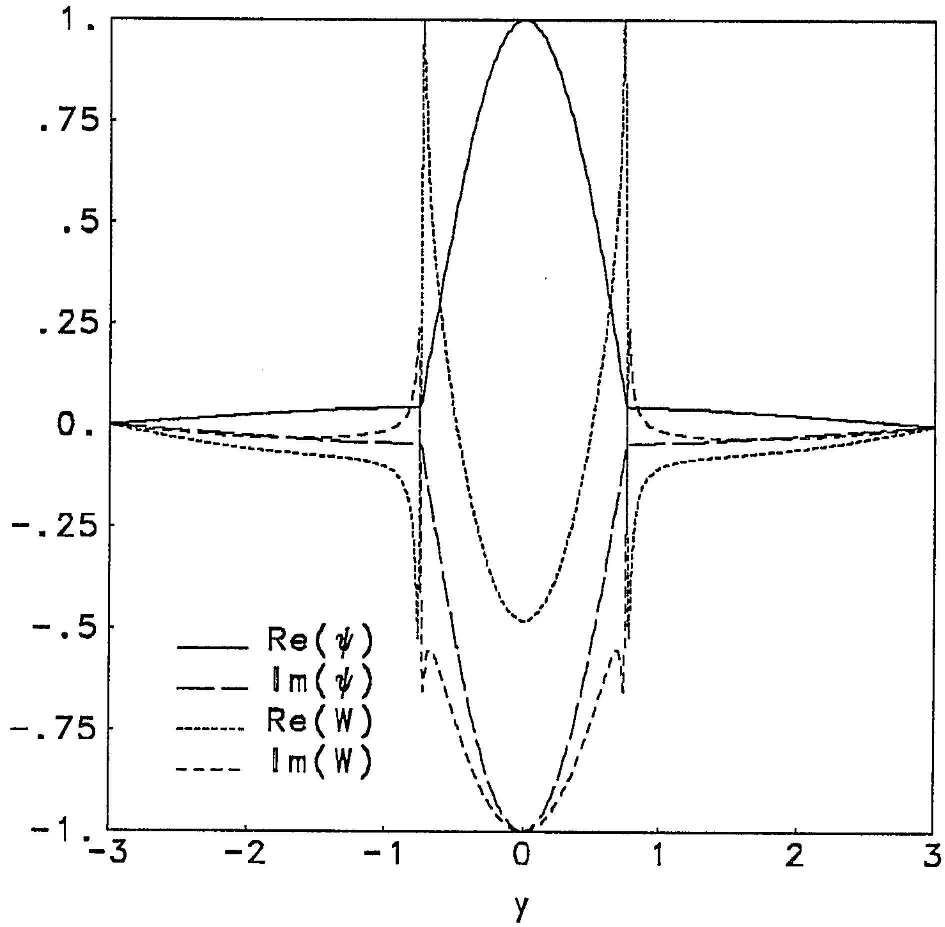

Fig. 2a

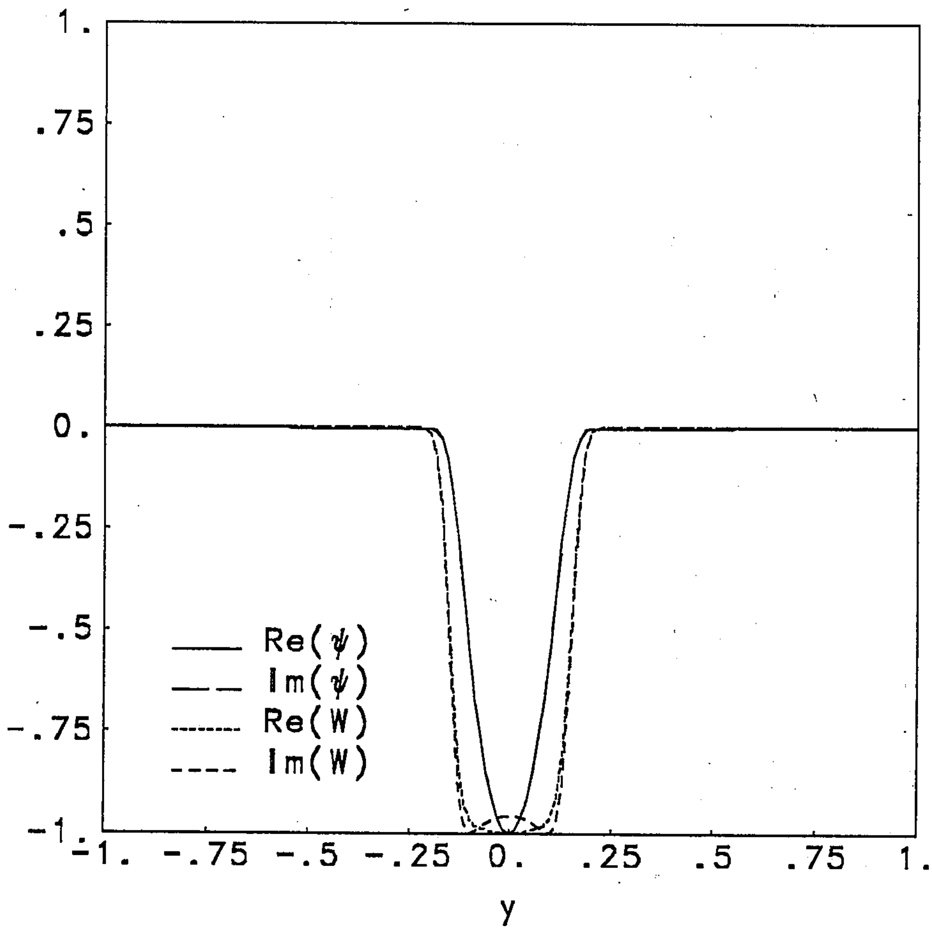

Fig. 2(b)

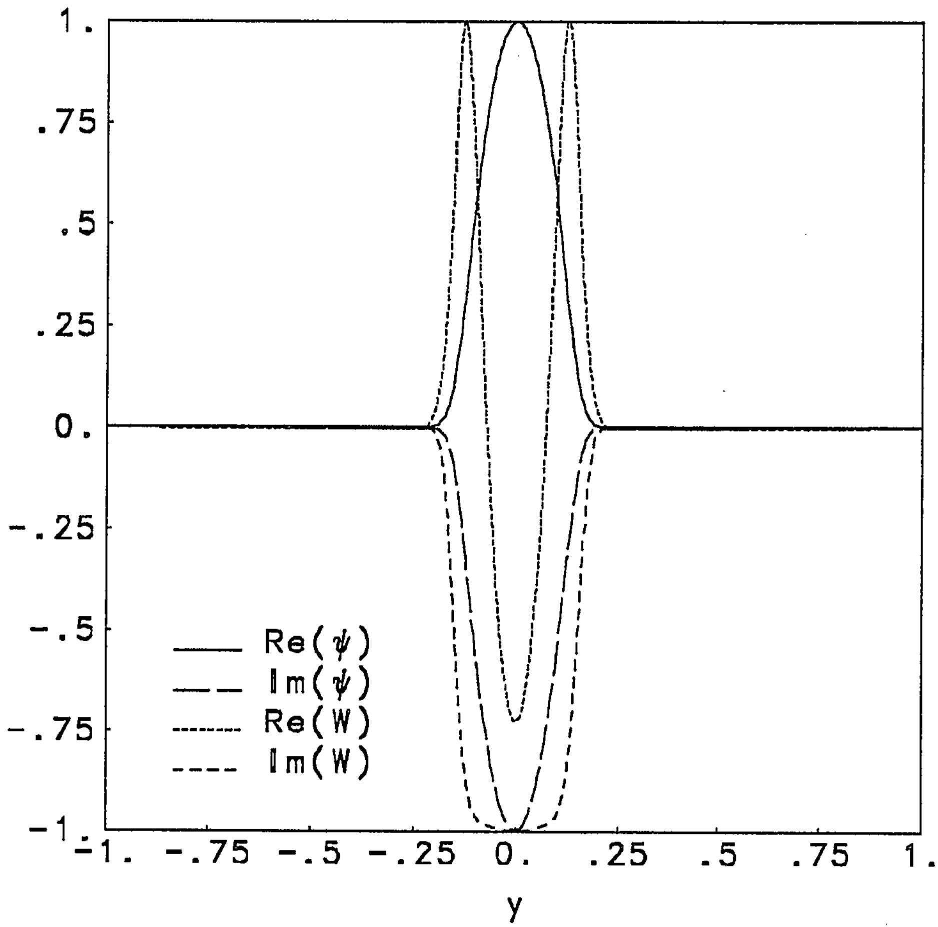

Fig. 2c

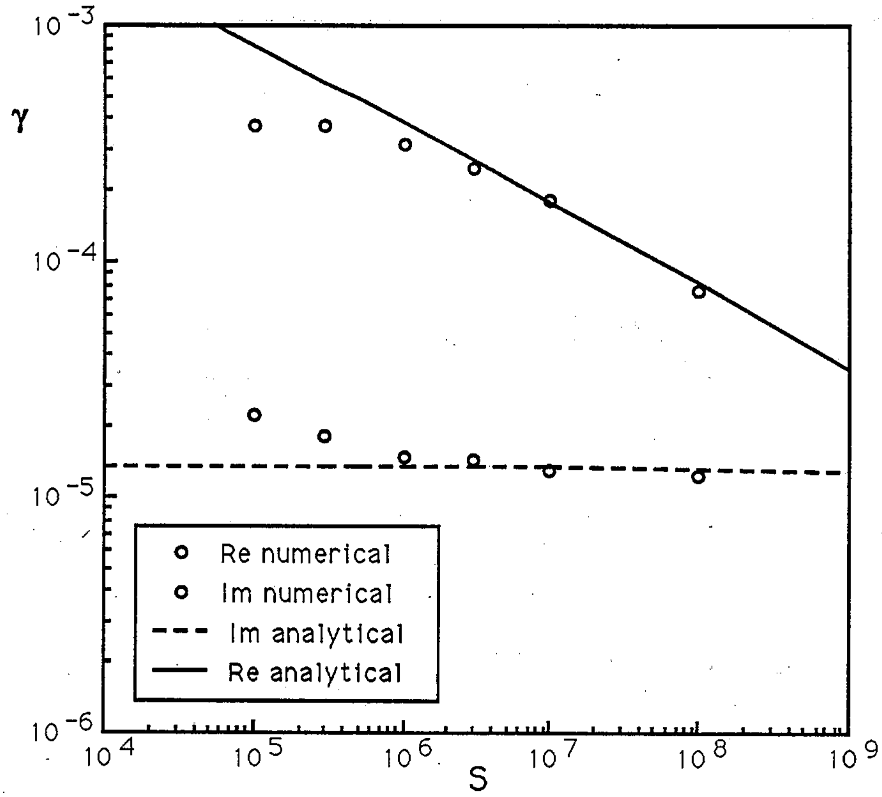

10 -3
10 -4
10 -5
10 -6
γ
Re numerical
Im numerical
Im analytical
Re analytical
10 4
10 5
10 6
10 7
10 8
10 9
S

Fig. 3a

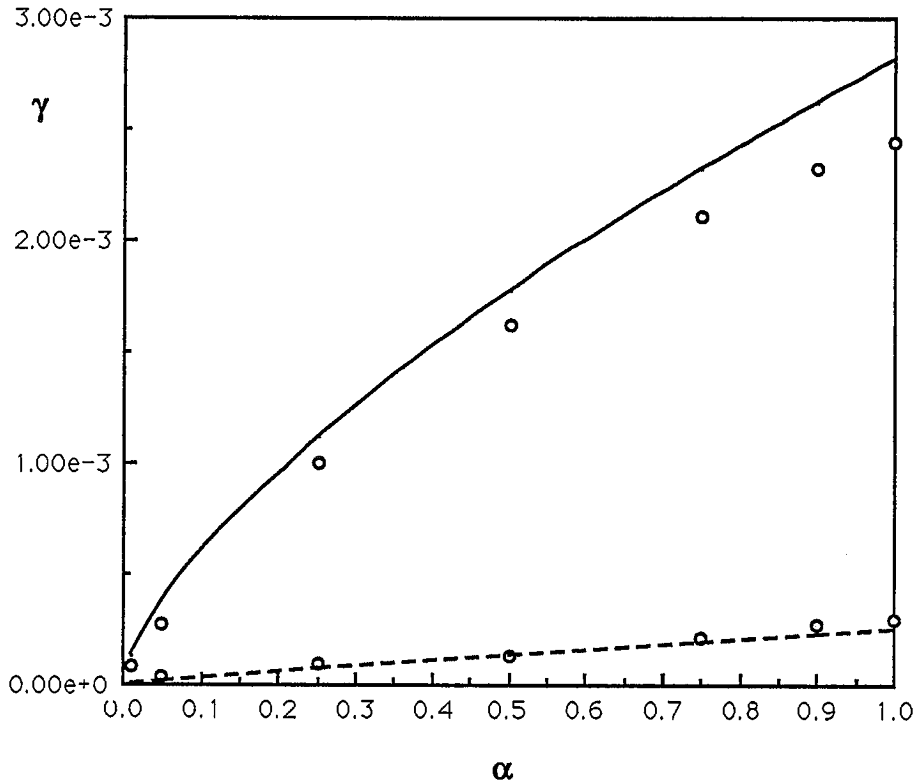

Fig. 3(b)

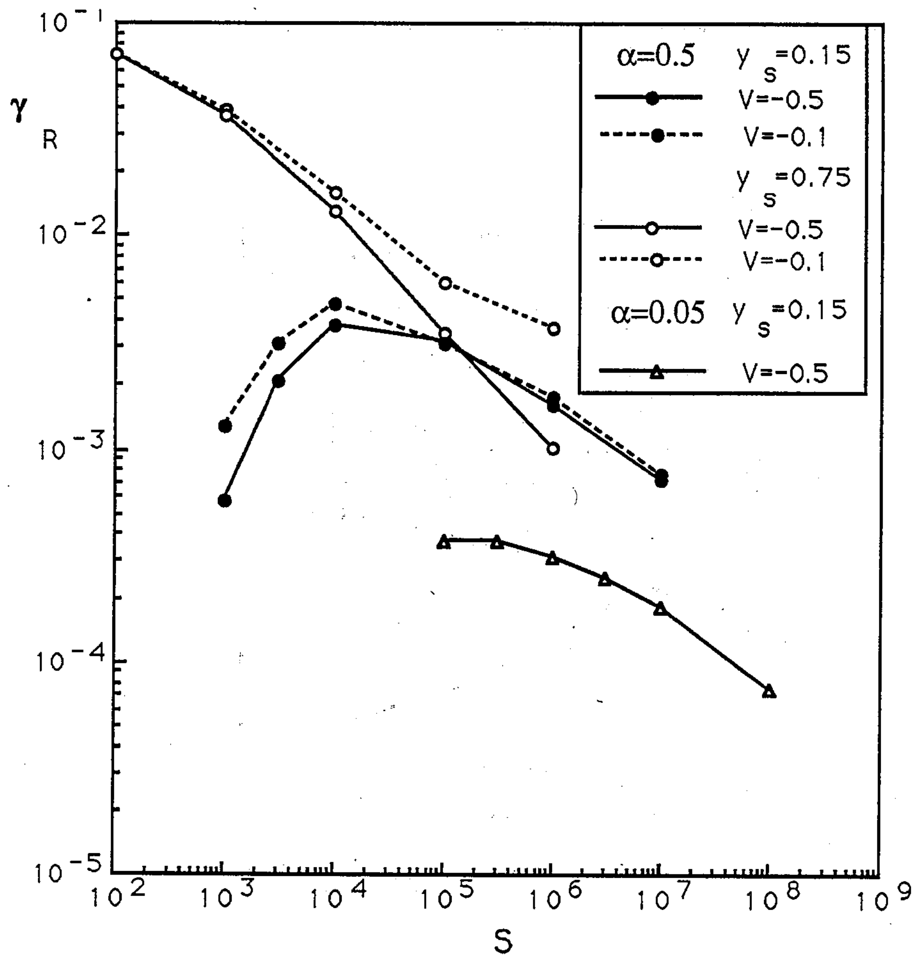

Fig. 4

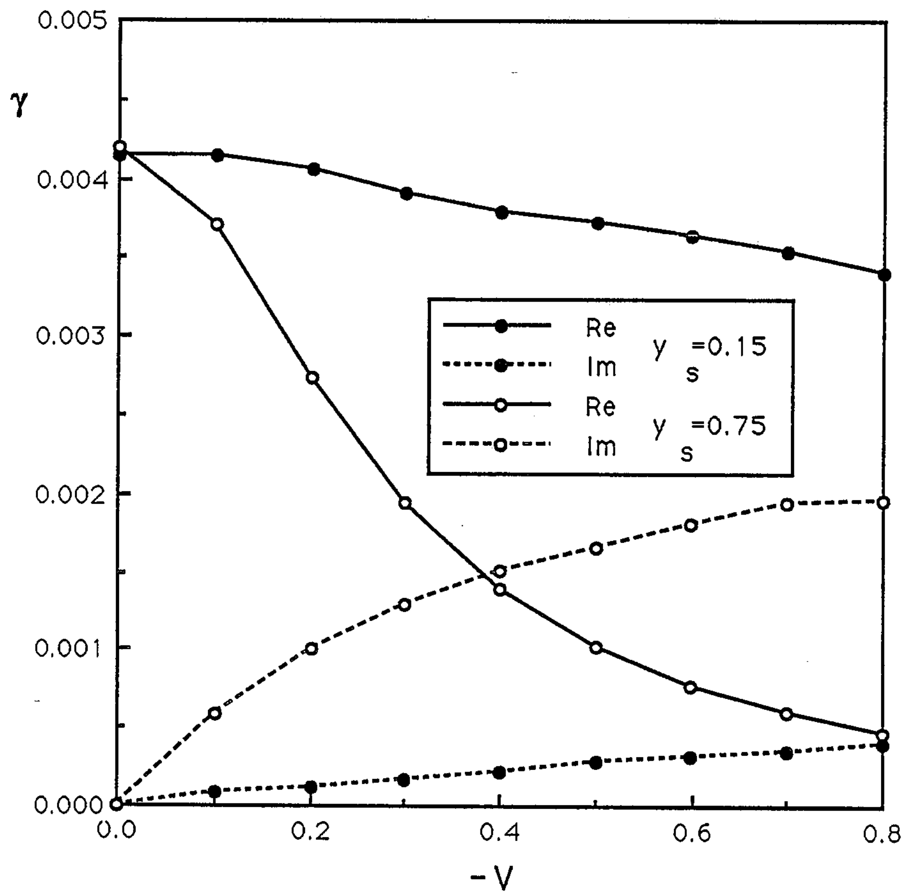

0.005
0.004
0.003
0.002
0.001
0.000
γ
0.0
0.2
0.4
0.6
0.8
-V
Re
Im
y s =0.15
Re
Im
y s =0.75

Fig. 5

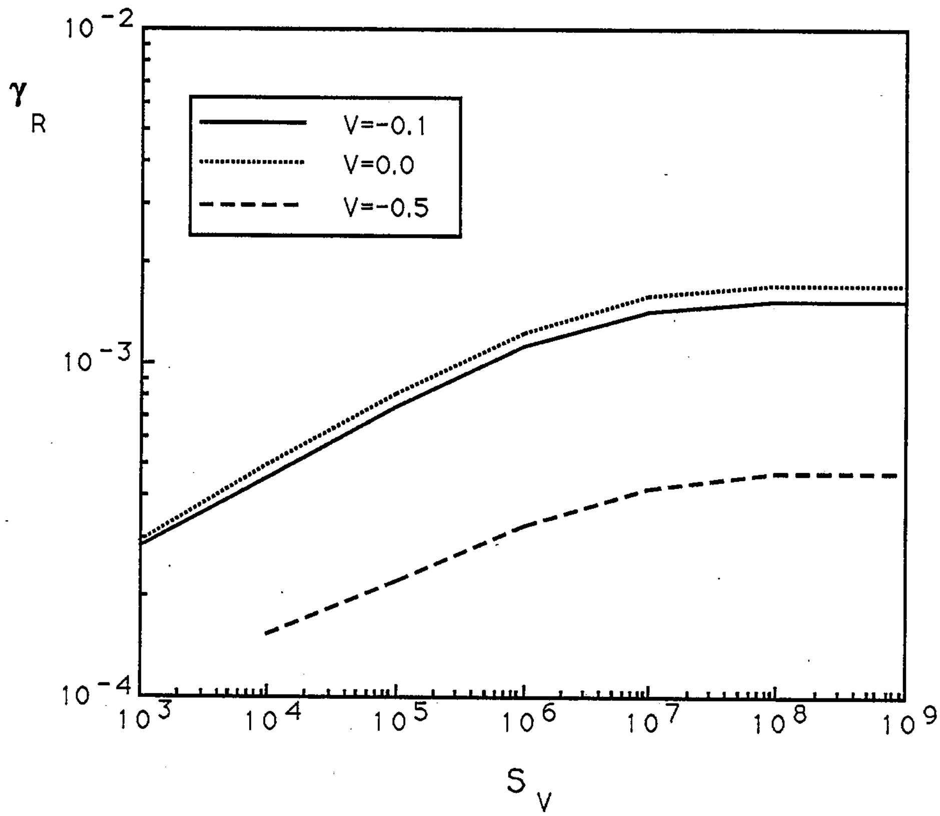

Fig. 6